Single image rain removal based on Multi-scale and channel attention mechanism

Qiuling Liu [1], Gang Zhou [2,*] and Zhenhong Jia [3]

1 College of Information Science and Engineering, Xinjiang University, Urumqi, 830046, China; l_qiuling@163.com
2 College of Information Science and Engineering, Xinjiang University, Urumqi, 830046, China; gangzhou_xju@126.com mail.com
3 College of Information Science and Engineering, Xinjiang University, Urumqi, 830046, China; jzhh@xju.edu.cn
* Correspondence: gangzhou_xju@126.com.

Abstract: Deep convolutional neural network (CNN) has shown their great advantages in the single image deraining task. However, most existing CNN-based single image deraining methods still suffer from residual rain streaks and details lost. In this paper, we propose a deep neural network including the Multi-scale feature extraction module and the channel attention module, which are embed in the feature extraction sub-network and the rain removal sub-network respectively. In the feature extraction sub-network, the Multi-scale feature extraction module is constructed by a Multi-layer Laplacian pyramid, and is then integrated multi-scale feature maps by a feature fusion module. In the rain removal sub-network, the channel attention module, which assigns different weights to the different channels, is introduced for preserving image details. Experimental results on visually and quantitatively comparison demonstrate that the proposed method performs favorably against other state-of-the-art approaches.

Keywords: Single image deraining; Multi-layer Laplacian pyramid; Multi-scale feature extraction module; Channel attention module.

1. Introduction

Rain streaks can severely degrade the image quality and affect the performance of computer vision tasks such as visual object detection, image semantic analysis and so on [1]. Single image deraining aims at recovering free image from a rainy image, and has attracted extensive research attention. Therefore, removing rain streaks from a single image is a meaningful task, which can improve the effect of subsequent processing tasks. However, there are still some problems have not been resolved. The foremost reason is the case that the density, shape, direction, and location of rain streaks are difficult to estimate. Meanwhile, the background image is damaged by rain streaks, and is difficult to restore. In this paper, we are dedicated to work out these problems.

In the past several decades, single image deraining methods can be roughly divided into the prior-based methods and the learning-based methods. The most significant distinction between these two types is that the former is handcrafted but the latter is learned automatically[2].

The prior-based methods mainly exploit the physical characteristics of rainy images as prior knowledge. Kang et al. adopt bilateral filters to decompose the image into high and low frequency components. And then, dictionary learning and sparse coding are introduced to decompose the high-frequency components into rain components and rainless components [3]. Huang et al. apply affinity propagation presentation to achieve clustering of image sub-blocks, and leverage the large variance of rainless sub-blocks to obtain high-frequency rainless components [4]. Xu et al. introduce the chromaticity characteristics of raindrops to obtain the guide image, which can filter the raindrop image to a free image [5]. Chen et al. take sparse representation to separate rain streaks from high-frequency components by the feature sets including directional gradient histograms, depth of field, and intrinsic colors [6]. Pan et al. merge the data-related network into the established iteration, learning a two-layer hierarchical prior method to study the problem of removing rain streaks [7]. Kim et al. propose to detect the rain pattern area by analyzing the rotation angle and aspect ratio of the elliptical core at each pixel [8]. The prior-based methods can improve the part of visibility, but the performance is not good as features are handcrafted.

In recent years, along with the excellent performance of convolutional neural network in image processing tasks, the learning-based methods have been extensively utilized in rain removal[9-19]. However, most of the learning-based methods do not implement sufficiently. In Figure 1, we display the consequences of advanced methods [9-11]. As shown in the first row of Figure 1, we can clearly see that current methods are sometimes difficult to remove the residual rain streaks on the face. In the second row, the texture information is vanished or blurred after removing the rain. As the variable size of rain streaks, it is difficult to describe the rain drops by a single scale feature map. And the rain streaks, which are highly overlapped with background, are usually failed to remove while recovering image details.

(a) JORDER[9] (b) RESCAN[10] (c) PReNet[11] (d)Original image

Figure 1. Visual comparison of some approaches on the problems of residual rain streaks and detail lost.

Recently, some researchers focus on Multi-scale features to describe the rain streaks. To exploit the complementary information of Multi-scale versions, many deep learning methods establish the Multi-layer pyramid architecture to make the rain removal more thorough. Fu et al. propose a lightweight pyramid network with shallow depth and simple framework. It processes the rebuilding task into multiple sub-problems and employs a series of parallel sub-networks to separately evaluate the rain streaks[20]. Jiang et al. design a Multi-scale progressive fusion network via the pyramid architecture and the attention mechanism. It combines a set of multi-scale features by the coarse-fusion module and the fine-fusion module[21]. Different from the existed methods, we propose a Multi-layer Laplacian pyramid architecture with a feature fusion (FF)module. This module is inspired by U-Net [22], which aims to combine the Multi-scale feature maps. To enhance the Multi-scale information, the original image is also concatenated into the output of the FF module. It shows a great advantage to the rain removal sub-network.

Lately, some novel methods demonstrate that the channel attention module can greatly improve results. For example, Li et al. take the Squeeze-to-Excitation (SE) module to assign different weights to different channels, and achieve better effects[10]. Deng et al. [8] propose a residual network, which combines the channel attention module and the residual module to make full use of spatial context information[23]. Wang et al. propose a novel spatial attention module to remove rain streaks[24]. It can be seen that the addition of channel attention module can effectively enhance the weight of crucial features, so as to preserve more details and improve image clarity. Different from the above methods, the SE module is only embedded behind the feature extraction residual (FER) module. As we found that the Multi-scale feature maps are redundant, the SE module can help us to determine the significance of different channels and assign different weights. In this paper, the architecture of network includes the feature extraction sub-network and the rain removal sub-network. The feature extraction sub-network is exploited to extract feature maps from the original images. The rain removal sub-network is utilized to deraining via long-short term memory (LSTM) [25], FER module, SE module primarily.

2. Materials and Methods

As shown in Figure 2, the Multi-scale and the channel attention module are important components in our network. The rain streaks are eliminated stage by stage. Our network consists of the input module, LSTM, FER module, SE module, and output module at each stage. And all the stages can be divided into the feature extraction sub-network and the rain removal sub-network. In the feature extraction sub-network, we design a Multi-layer Laplace pyramid and utilize the FF module to get Multi-scale feature maps. In the rain removal sub-network, we use LSTM, FER module, SE module to remove rain streaks. With LSTM, we can take full advantage of the effective information in prior stages. The FER module used in each stage can benefit us extract deep features and acquire more significant information. At the same time, we incorporate the SE module that assigns different weights to various feature channels in term of their inter-dependencies. Then, we will introduce each module and loss function around the above each stage.

2.1. Feature extraction sub-network

In outdoor scenes, the diameter of raindrops is generally 10μm~1000μm. Therefore, the motion blur of raindrops generates rain streaks, which usually occupies a dozen to hundreds of pixels on the image. As we can know, rain streaks have various directions and shapes. It is far from enough to depend on a single scale feature extraction module. To solve the above problem, we propose a Multi-layer Laplacian pyramid method.

To begin with, we define Gaussian convolution kernel. Then, successive convolution and maxpooling operations generate a Gaussian pyramid. Finally, the Multi-layer Laplacian pyramid is produced via the relationship between Gaussian and Laplacian operations. This process can be formulated as:

$$G_n(X) = Mp(Conv_{Gau}(X)) \tag{1}$$

where X are the rainy images, $G_n(X)$ is the Gaussian pyramid, $n=1, \ldots, N-1$. Mp is the maxpooling operation of 2*2 window size. $Conv_{Gau}$ are three 3 * 3 Gaussian convolution kernels. Through the above process, the input rainy image is decomposed into a group of Gaussian pyramids with different scales and resolutions. And then, the Multi-layer Laplacian pyramid is generated by the next operation. The calculation process can be expressed as：

$$L_n(X) = G_n(X) - Upsample(G_{n+1}(X)) \tag{2}$$

where $Upsample$ adopts the nearest interpolation processing method. $L_n(X)$ is the Laplacian pyramid. It can eliminate the redundant information and preserve the unique features of the Gaussian pyramid. Meanwhile, the Laplacian pyramid contains different scales of rain streaks and details that are helpful to the rain removal sub-network.

The background information can be completely extracted at the top layer of $L_n(X)$ while the other layers include different scales, features and resolutions, which are very

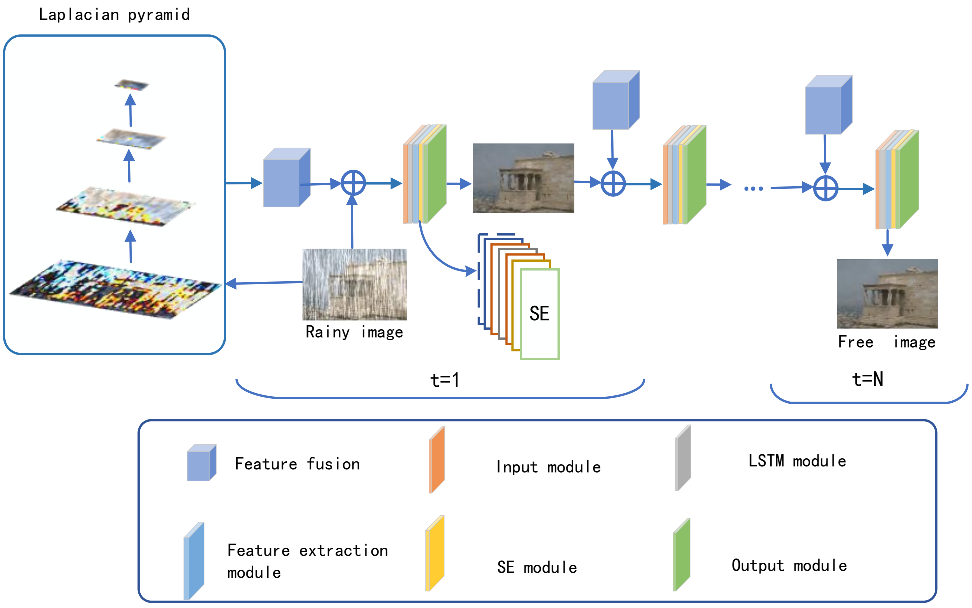

Figure 2. The overall framework of multi-scale, multi-channel attention module network.

similar to the physical properties of the rain streaks. Therefore, we can conclude that the architecture of Multi-layers pyramid is very important in the process the rain streaks separation. In order to achieve the crucial performance of multi-layers Laplacian pyramid, it is necessary to fuse the features of each layer via feature fusion operation. Inspired by U-Net [22], the FF module is shown in Figure 3. $L_{n+1}(X)$ means nearest neighbor interpolation up-sample that aims to prepare for the next step. $L_n(X)$ means a 3*3 convolution operation for extracting features. After the above operations, we can attain intermediate feature maps. In general, the FF module is utilized to integrate information from different scales.

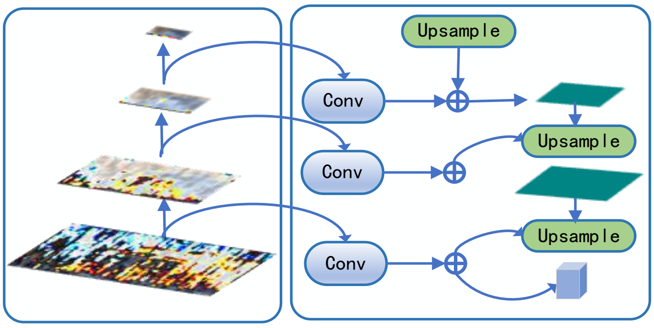

Figure 3. The unfolded architecture of FF module.

2.2. Feature extraction sub-network

Considering that the rain streaks are randomly distributed in three-dimensional space, it leads to the rain streaks of different motion tracks overlapped. So, it is extremely difficult to remove rain streaks completely. In [10, 11], the multi-stage iterative structure is utilized to eliminate the rain streaks and to achieve the desired results. In view of the previous experience, our method also references this kind of rain removal structure.

For a rainy image, our method generates a feature map using nearest neighbor interpolation up-sample and the convolution kernel. Next, the outputs of feature extraction sub-network go through the rain removal sub-network. Firstly, we take the multi-scale feature map and the original image as input via initial convolution layer to extract the shallow features. Secondly, to exploit the effective information of the previous stage, we incorporate LSTM into the model that can preserve the necessary information and enhance the connection of each stage. Thirdly, five residual modules are appended to extract the deep features, which mainly include important information about the original image.

By multiplying weights learned by the SE module, the feature maps calculated by convolution are updated accurately. Finally, the rain removal results are output via 3 * 3 convolution kernels. In summary, the whole rain removal process is divided into six stages, and the above modules are applicable to each stage. The input of the first stage is completely different from that of the other five stages. The input of the first stage is the connection of the multi-scale feature map and the original image, while the other stages is the connection between the multi-scale feature maps and the output of the previous stage.

2.2.1. FER module

The existing part of rain removal methods [9-11]exploit residual module, because it is helpful to extract deep features and obtain more details of the original image. In this paper, the FER module is composed of five recursive parts, each of which extracts the deep feature of the original image via 64 channels. The N-th stage of the FER module process is shown as follows:

$$x^t = F_{in}(x^{t-1}, L_n(x)) \tag{3}$$

$$s^t = F_{LSTM}(s^{t-1}, x^t) \tag{4}$$

$$x^N = F_{\mathrm{Res}}(s^t) \tag{5}$$

where s^t is the output of the LSTM. x^t is the input of the current stage, x^N is the output of the FER module, F_{in} is the input module, F_{LSTM} is the LSTM operation. F_{Res} is the FER module operation. The module extracts the deep characteristics of input completely, and plays an irreplaceable role in the process of rain removal.

2.2.2. SE module

The influence of different channels is distinct in rain removal and preserving image details. The convolution kernels implicitly introduce weights for each channel, but these implicit weights are not particular for each image. As a result, we introduce the SE module that allocates different weights to different channels. The SE module can be embedded into the network to realize the channel attention mechanism [26]. In this paper, the SE module receives the output of the FER module, that can fit the feature association and assign higher weights to important channels. So, it further optimizes the rain removal effect. The inference process of the SE module is as follows:

$$SE_{out} = F_{SE}(x^N) \tag{6}$$

where F_{SE} is the calculation process of the SE module, SE_{out} is the output of the SE module. The SE module receives the output from the FER module and assigns weights by global pooling layer, fully connected layers and sigmoid function. By multiplying the output of the SE module, feature maps are re-weighted to keep image details.

2.3. Loss function

Mean square error (MSE) is a commonly used loss function in rain removal. However, there are still some problems. For example, it can cause image blurred, excessive smoothing, loss of high-frequency components [27]. According to[11, 28], the structural similarity (SSIM) loss function is exploited to training process. The SSIM loss takes brightness, contrast and structure into account, which is very consistent with human visual perception. Meanwhile, compared with MSE, SSIM has better effect on texture, detail and edge.

$$L_{-SSIM} = -SSIM(x^n, x^{target}) \tag{7}$$

where x^n is the output image, x^{target} is the ground truth image, SSIM[28] explains as follows:

$$SSIM(x, y) = \frac{(2\mu_x\mu_y + C_1)(2\sigma_{xy} + C_2)}{(\mu_x^2 + \mu_y^2 + C_1)(\sigma_x^2 + \sigma_y^2 + C_2)} \tag{8}$$

where μ is variance, σ is covariance.

3. Results

In this section, we implement extensive experiments on public synthetic and real image datasets to compare the recovery performance of our proposed network with state-of-the-art deraining methods. These methods include that LPNet [20], JORDER [9], DID-MDN [13] and PReNet [11]. Meanwhile, we verify the effectiveness of the multi-layer Laplacian pyramid module and the SE module via ablation study. In this paper, we utilize PSNR and SSIM to analyze the deraining results.

In this paper, our entire network is implemented by Pytorch framework and trained on a PC equipped with one GPU. The experimental parameters are set as follows. The batch size is 8, and the epoch is 90. The Adam algorithm optimizes the model with an initial learning rate 1e-3. When up to 30, 50 and 80 epochs, the learning rate is declined to 20%.

3.1. Ablation study

To analyze the significance of each component in our proposed network, we have performed ablation study with / without each specific component. We focus on two components: the multi-layer Laplacian pyramid and the SE module.

3.1.1. Analysis of the Multi-layer Laplacian pyramid

In this paper, ablation study is implemented to verify the influence of the number of layers of the Multi-layer Laplacian pyramid. As we know in [20, 21], the pyramid architecture is set to 3 and 5 layers respectively. Therefore, on the Rain100H datasets, we tested the influence of the number of layers on rain removal performance and their average test time. It can be seen from Table 1 that the PSNR and SSIM have been improved by introducing Multi-layer Laplacian pyramid. The PSNR increased by 0.31, and the SSIM increased from 0.899 to 0.9046. It can be observed that with the increase of Multi-layer Laplacian pyramid layers, the rain removal performance will be advanced. However, the average test time will be increased at the same time. The average test time of the 5-layer pyramid is 0.01 second longer than that of the 3-layer pyramid. It can be seen from the experiment that the more layers, the more scene information it contains. Considering the compromise between the performance and the computing efficiency, we define the number of Laplacian pyramid layers to 4.

Table 1. Performance comparison of pyramid layers.

Layers	3 layers	4 layers	5 layers
PSNR	29.50	29.63	29.76
SSIM	0.9026	0.9033	0.9046
Average time	0.1250s	0.1259s	0.1348s

3.1.2. Analysis of the multi-layer Laplacian pyramid

The SE module is embedded behind the FER module to learn the weights of the channels in the purpose of feature selection. As can be seen from Table 2, the PSNR and SSIM have been improved. Among them, PSNR is increased by 0.35, and SSIM is also increased to 0.9016. Meanwhile, our methods can well preserve more realistic and credible image details with the SE module. It can be observed in Figure 4 (b) that the edges of characters in the image become blurred and defected without SE module. As can be seen from Figure 4(c), compared with the rain-removing image without SE module, it is obvious that the image is more realistic and clarity.

Table 2. Performance comparison of pyramid layers.

Image quality index	Without SE	With SE
PSNR	29.45	29.80
SSIM	0.8990	0.9016

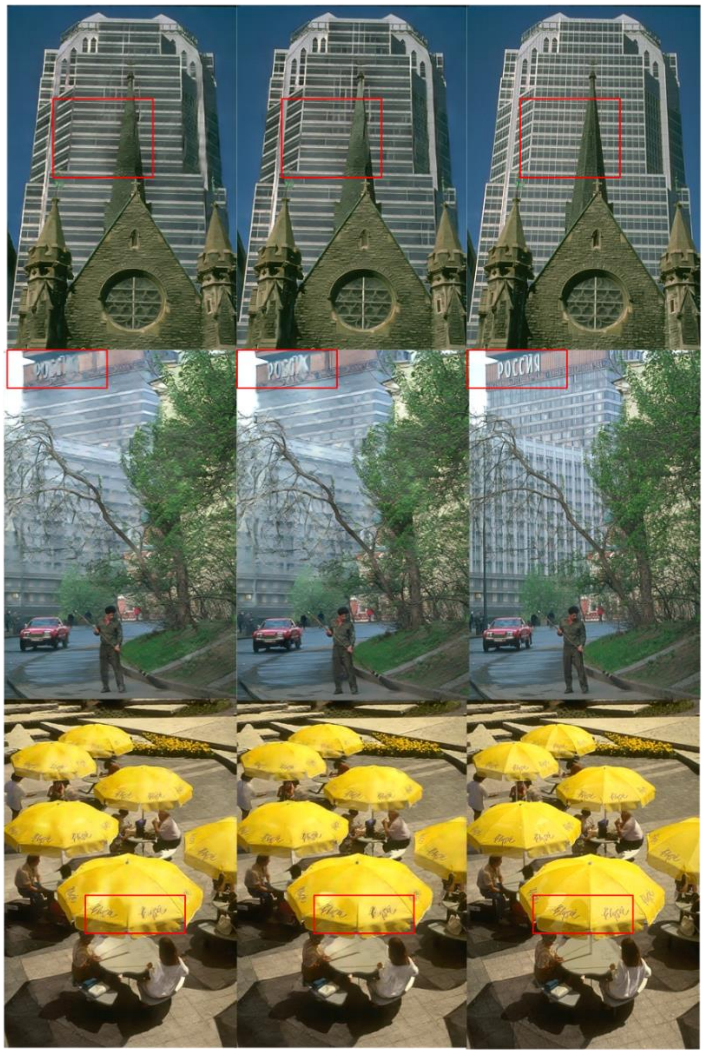

(a)Without SE module (b) With SE module (c) Ground Truth

Figure 4. Comparison of experimental effects between with SE module and without SE module.

3.2. Comparisons with State-of-the-arts

In this section, we evaluate our algorithm with a few excellent methods on both synthetic datasets and real images. On synthetic datasets, we compare with a series of the rain streaks removal methods: (a) LPNet [20] (b)JORDER [9], (c)DID-MDN [13], (d)PReNet [11]. And also, we compare with LPNet [20] and PReNet[11] on the real images.

3.2.1. Synthetic datasets

Comparative experiments are implemented on the synthetic datasets Rain100H and Rain100L, and the results are presented in Table 3. It can be seen from Table 3 that the experimental results of this algorithm are better than the existing advanced algorithms obviously. LPNet [20] is a network to remove rain streaks by constructing Laplacian pyramid. It declares the PSNR and SSIM values on the Rain100H are 23.74 and 0.81, which is lower than our results. And also, our method improves PSNR by 4.06 and SSIM by 0.0734 compared with JORDER [9]. Although DID-MDN [13] and PReNet [11] can achieve quite well rain removal results in some ways, our network is better that can both preserve the original image details and remove the rain streaks as far as possible from the input. We display the visualization effect compared with existing algorithms on the dataset Rain100H on Figure 5. It can be observed in Figure 5(a) that LPNet [20] cannot remove rain streaks under heavy rain conditions, and the effect of rain removal is not satisfactory. From Figure 5(b) and (c), it can be seen that the DID-MDN [13] and JORDER[9] networks can remove some the rain streaks. However, there are still some residuals, especially when the rain streaks are overlapped with the image background. It can be seen from Figure 5(d) that the PReNet [11] network is better than the DID-MDN [13] and JORDER [9] networks in terms of rain removal effect and clarity, but there are still a small amount of residual rain streaks and loss of details. Compared with the above algorithm, our method can not only remove the rain streaks very effectively, but also keep the details of the image while image deraining.

Table 3. Comparative experiments on the synthetic data set.

Datasets	LPNet [20]	DID-MDN [13]	JORDER[9]	PReNet[11]	ours
Rain100H	23.74/0.81	17.35/0.524	26.54/0.835	29.45/0.8991	30.06/0.9084
Rain100L	34.26/0.95	25.23/0.741	36.61/0.963	37.48/0.9792	38.50/0.9830

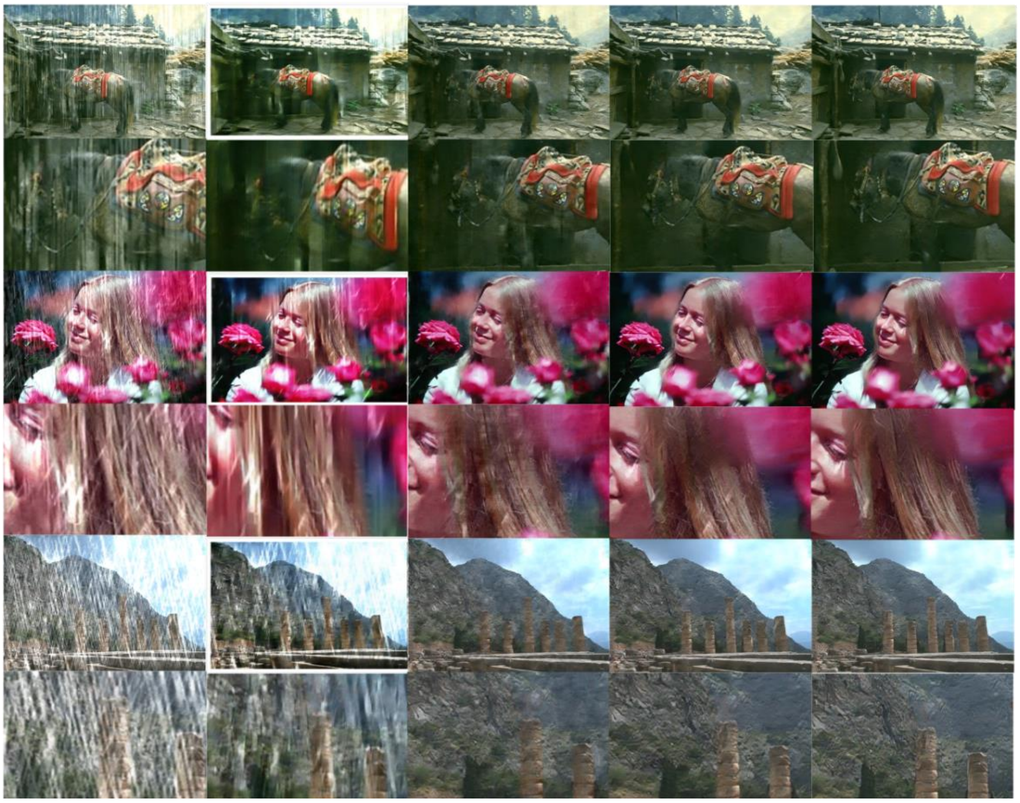

(a) LPNet [20] (b) DID-MDN[13] (c) JORDER[9] (d) PReNet[11] (d) ours

Figure 5. Comparison of experimental results with existing algorithms on the Rain100H

3.2.2. Real images

Nowadays, most rain removal algorithms have better results on synthetic datasets, but they do not do anything well on real images. To further validate the effectiveness of our method on removing rain streaks and retaining details, we conducted experiments on real images, as shown in Figure 6. Compared with our methods, the LPNet [20] and PReNet [11] still suffered the problem of blurred background and vanished details. In a word, our method has excellent performance on real images, which can effectively remove the rain streaks and retain more details of the image.

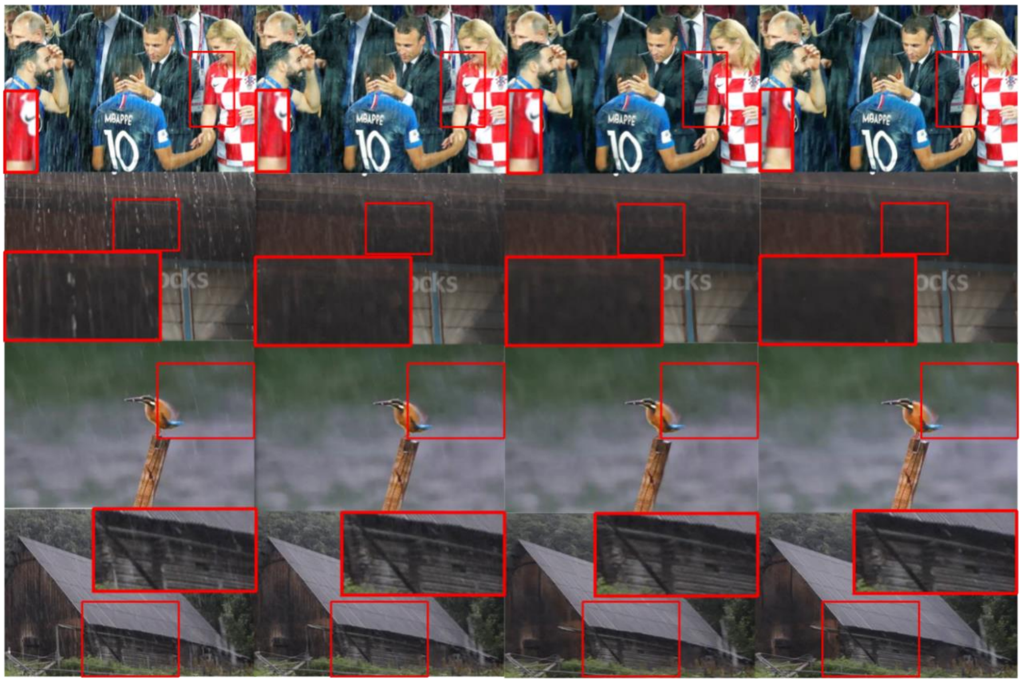

(a) Rainy images (b) LPNet [20] (c) PReNet[11] (d) ours

Figure 6. Experimental results of comparison with existing algorithms on real images

4. Discussion

In this paper, we propose a deep convolution neural network algorithm based on the multi-scale feature and the channel attention mechanism. The main contributions of this paper are as follows.

(1) We propose a Laplacian pyramid with self-defined Gaussian kernel, which extracts the multi-scale feature maps of rainy image. The FF module is introduced to integrate these feature maps in a complementary manner.

(2) The SE module is added into the rain removal sub-network to figure out the importance of different channels. It can completely retain and enhance the important feature channels, and recovers the image details.

(3) We verify the effectiveness of the Laplacian pyramid and the SE module by ablation study. And experimental results show that our approach can obtain superior performance compared with the previous state-of-the-art methods both qualitatively and quantitatively on various datasets.

5. Conclusions

In this paper, we propose a single image rain removal method based on the Multi-scale feature and the channel attention mechanism. We evaluate the rain removal performance of our algorithm by comparing with some existing methods. It can conclude that our method is more efficient in deraining on Rain100H and Rain100L. Meanwhile, we conducted analysis on real images. It turns out that our method is more effective in preserving the original image details and removing the rain streaks as much as possible. The above experiments verified that the Multi-scale feature which is extracted from the Multi-layer Laplacian pyramid, can greatly deal with the problem of residual rain streaks. The

SE Module retains more details via feature selection to make the image realistic. In summary, the Multi-layer Laplacian pyramid and SE module behind FER module skillfully make uses of the characteristics of the rain streaks, which greatly improves the rain removal effect.

Author Contributions: Based on the Multi-scale feature and the channel attention mechanism, we propose a single image rain removal method. The Multi-scale feature maps were obtained via the Multi-layer Laplace pyramid and FF module. LSTM can enhance the connection between stages. The FER module extracts deep features and acquire more significant information. The SE module re-weight for feature maps. Compared with state-of-the-art approaches, our proposed algorithm has a great improvement, in preserving detail and enhancing clarity. Q.L. and G.Z. completed previous work. Q.L., G.Z. and Z.J. designed the architecture of network. Q.L. and G.Z. designed the experimental section and implemented analysis. Q.Y., Q.L., G.Z. and Z.J. finished writing this paper. All authors have read and agreed to the published version of the manuscript.

Funding: The work supported by National Natural Science of Foundation of P.R. China(61603323，U1803261), Xinjiang University Doctoral Research Startup Fund Project.

Conflicts of Interest: The authors declare no conflict of interest.

References

1. Garg Kshitiz and N.S. K., *Vision and Rain.* International Journal of Computer Vision, 2007. **75**: p. 3-27.
2. Hong Wang, et al., *A Survey on Rain Removal from Video and Single Image.* arXiv preprint arXiv:1909.08326, 2019: p. 1-13.
3. Li-Wei Kang, Chia-Wen Lin, and Y.-H. Fu., *Automatic single-image-based rain streaks removal via image decomposition.* IEEE Trans Image Process, 2012. **21**(4): p. 1742-55.
4. De-An Huang, et al., *Self-Learning Based Image Decomposition With Applications to Single Image Denoising.* IEEE Transactions on Multimedia, 2014. **16**(1): p. 83-93.
5. Jing Xu, et al., *Removing Rain and Snow in a Single Image using Guided Filter.* IEEE International Conference on Computer Science and Automation Engineering 2012: p. 304-307.
6. Duan-Yu Chen, Chien-Cheng Chen, and L.-W. Kang., *Visual Depth Guided Color Image Rain Streaks Removal Using Sparse Coding.* IEEE Transactions on Circuits and Systems for Video Technology, 2014. **24**(8): p. 1430-1455.
7. P . Mu, J.C., R. Liu, X. Fan, and Z. Luo., *Learning bilevel layer priors for single image rain streaks removal*. IEEE Signal Processing Letters. 2019.
8. Jin-Hwan Kim, et al., *Single-image deraining using an adaptive nonlocal means filter.* IEEE International Conference on Image Processing, 2013: p. 914–917.
9. Wenhan Yang, et al., *Deep Joint Rain Detection and Removal from a Single Image*, in *IEEE Conference on Computer Vision and Pattern Recognition* 2017. p. 1685-1694.
10. Xia Li, J.W., Zhouchen Lin,Hong Liu, Hongbin Zha., *Recurrent Squeeze-and-Excitation Context Aggregation Net for Single Image Deraining.* Internaltional Conference on Computer Vision and Pattern Recogintion, 2018: p. 1-16.
11. Dongwei Ren, et al., *Progressive Image Deraining Networks A Better and Simpler Baseline.* Internaltional Conference on Computer Vision and Pattern Recogintion, 2019: p. 1-11.
12. Xueyang Fu, et al., *Removing rain from single images via a deep detail network.* Internaltional Conference on Computer Vision and Pattern Recogintion, 2017: p. 3855-3863.
13. He Zhang and V.M.P. . *Density-aware Single Image De-raining using a Multi-stream Dense Network.* Internaltional Conference on Computer Vision and Pattern Recogintion, 2018: p. 1-10.
14. Rajeev Yasarla and V.M. Patel., *Uncertainty Guided Multi-Scale Residual Learning-using a Cycle Spinning CNN.* Internaltional Conference on Computer Vision and Pattern Recogintion, 2019: p. 1-10.
15. Wei Wei, et al., *Semi-supervised Transfer Learning for Image Rain Removal.* Internaltional Conference on Computer Vision and Pattern Recognition, 2019: p. 1-10.

16. Zheng Wang, Jianwu Li, and G. Song., *DTDN: Dual-task De-raining Network*, in *Proceedings of the 27th ACM International Conference on Multimedia*. 2019. p. 1833-1841.
17. Jingwei He, et al., *Single Image Deraining with Continuous Rain Density Estimation.* arXiv:2006.03190v1 2020: p. 1-11.
18. Wenhan Yang, et al., *Joint Rain Detection and Removal from a Single Image with Contextualized Deep Networks.* IEEE Trans Pattern Anal Mach Intell, 2020. **42**(6): p. 1377-1393.
19. Yulong Fan, Rong Chen, and B. Li., *Multi-Task Learning Enhanced Single Image De-Raining.* Internaltional Conference on Computer Vision and Pattern Recogintion, 2020: p. 1-15.
20. Xueyang Fu, et al., *Lightweight Pyramid Networks for Image Deraining.* IEEE Trans Neural Netw Learn Syst, 2018. **31**(6): p. 1794-1807.
21. Kui Jiang, et al., *Multi-Scale Progressive Fusion Network for Single Image Deraining.* Internaltional Conference on Computer Vision and Pattern Recogintion, 2020: p. 1-10.
22. Olaf Ronneberger, Philipp Fischer, and T. Brox., *U-Net: Convolutional Networks for Biomedical Image Segmentation.* IEEE International Conference on Computer Vision, 2015: p. 1-8.
23. Sen Deng, et al., *Detail-recovery Image Deraining via Context Aggregation Networks.* Internaltional Conference on Computer Vision and Pattern Recogintion, 2020: p. 14560-14569.
24. Tianyu Wang, et al., *Spatial Attentive Single-Image Deraining with a High Quality Real Rain Dataset.* Internaltional Conference on Computer Vision and Pattern Recogintion, 2019: p. 1-10.
25. Xingjian Shi, et al., *Convolutional LSTM Network: A Machine Learning Approach for Precipitation Nowcasting.* Internaltional Conference on Computer Vision and Pattern Recognition, 2015: p. 1-12.
26. Jie Hu, et al., *Squeeze-and-Excitation Networks.* Internaltional Conference on Computer Vision and Pattern Recogintion, 2019: p. 1-13.
27. Zhao, H., et al., *Loss Functions for Image Restoration With Neural Networks.* IEEE Transactions on Computational Imaging, 2017. **3**(1): p. 47-57.
28. Zhou Wang, et al., *Image Quality Assessment: From Error Visibility to Structural Similarity.* IEEE Trans Image Process, 2004: p. 1-15.